

# THERMAL STATE, THERMAL MODELLING, AND HYDROCARBON GENERATION IN THE TARANAKI BASIN, NEW ZEALAND

P A Armstrong<sup>1</sup>, D S Chapman<sup>1</sup>, R H Funnell<sup>2</sup>, R G Allis<sup>2</sup>, P J J Kamp<sup>3</sup>

<sup>1</sup>Department of Geology and Geophysics, University of Utah, Salt Lake City, UT, USA

<sup>2</sup>Institute of Geological Sciences, Lower Hutt, New Zealand

<sup>3</sup>Department of Earth Sciences, University of Waikato, Hamilton, New Zealand

## Abstract

The present-day thermal state of the Taranaki Basin has been determined using a reassessment of bottom-hole temperatures, new thermal conductivity data, and new porosity/depth relations. An average thermal gradient of 29° C/km characterises much of the basin. Present-day heat flow through the sedimentary section ranges between about 50 and 70 mWm<sup>-2</sup>.

Heat flow, vitrinite reflectance, coal rank, and apatite fission track ages were used to constrain thermal history models for selected wells. Our one-dimensional numerical simulations include the transient thermal effects of sedimentation, erosion, lithospheric thinning/thickening, and overthrusting. Relative amounts and rates of hydrocarbon generation are computed from the simulated thermal histories for different regions of the basin using an Arrhenius first order, parallel reaction approach.

We have investigated two end-member thermal models: 1) a simple, constant upper mantle heat flow throughout the Cenozoic basin history with no predepositional rifting and erosion, and 2) constant upper mantle heat flow, with the thermal effects of Mesozoic crustal thickening, erosion, and syndepositional rifting. The latter results in 30% higher initial heat flow (at 75 Ma) that imparts long-lived transient thermal signals. Modelling results indicate that the high initial heat flow affects only the deepest source rocks (Rakopi Formation), especially where they are thick and were buried to depths of greater than about 2.5 km prior to 60 Ma, as in Kapuni Deep-1 and McKee-1 regions where generation and expulsion may have been as early as early Paleocene.

In the Western Platform region, all potential source rocks are probably immature, with generation amounts sufficient for maturation being reached only in the last one million years for most of the source rocks and as early as the Eocene for the deepest source rocks. In the Maui-4 region, temperatures and generation rates were greatest about 5–10 Ma, but decreased about 5 Ma coincident with structural inversion; temperatures are presently too low for significant oil expulsion (less than 120° C) in Maui-4.

Oil generation and expulsion in the eastern Taranaki region is dominated by Miocene to Recent tectonics. In the Kapuni field, the Rakopi section is overmature, with the shallower Paleocene–Eocene source rocks just entering the expulsion window. In contrast, Kaimiro-1 and McKee-1 regions both probably had significant generation and expulsion from the underlying Rakopi and shallower Paleocene–Eocene sections starting about 10 Ma. Temperatures in the Paleocene–Eocene rocks presently are great enough for oil expulsion, especially at Kaimiro-1 where present-day surface heat flow is relatively high.

## Introduction

The Taranaki Basin is located on the western margin of New Zealand (figure 1) and lies adjacent to the Australian/Pacific plate boundary where it changes from subduction along the Hikurangi Trench to dextral-oblique displacement along the Alpine Fault to the southwest. It is an active-margin basin that owes much of its origin to the evolving plate interactions of the area. The structural and stratigraphic history of the Taranaki Basin has been reviewed extensively (e.g. Pilaar and Wakefield, 1978; Knox, 1982; King and Robinson, 1988; Thrasher, 1990a; King, 1991; King and Thrasher, 1992), but generally includes crustal thickening, uplift, and erosion during the Permian to mid-Cretaceous, Late Cretaceous rifting, early-mid Cenozoic subsidence, and Miocene to recent extension, subsidence, volcanism,

thrusting, and structural inversion in its southern and eastern parts.

The Taranaki Basin provides the only known commercial hydrocarbon reserves in New Zealand, with most of these derived from coals and carbonaceous shales deposited in coastal plain swamps during the Late Cretaceous (Pakawau Group) and Paleocene–Eocene (Kapuni Group) (King and Thrasher, 1992; Killups et al., in press). A generalized stratigraphic cross-section for the Taranaki basin is shown in figure 2. Reservoir rocks generally are considered to be mainly within the Kapuni Group (Pilaar and Wakefield, 1978; Robinson and King, 1988; King, this volume). The region between the Western Platform and the Taranaki Fault Zone (figure 1) is filled with Miocene and younger muds and silts and some sandy fan deposits, some of which are known hydrocarbon reservoirs (Robinson and King, 1988).

Heat flow values calculated by Pandey (1981) suggest values of 80–100 mWm<sup>-2</sup> in the central and northern troughs, and lower values in the southern regions. Despite these moderately high heat-flow values, relative to comparable basins in other parts of the world, and large sediment thicknesses, the Taranaki Basin kerogens are regarded as being relatively immature. To date, little quantitative evaluation of the thermal and hydrocarbon generation histories for areas of the Taranaki Basin has been undertaken. Most maturation studies have taken into account maturity indicators, such as coal rank and vitrinite reflectance, to deduce past burial depths and temperatures based on present temperatures and geotherms (e.g. Sykes et al., 1992). Their study did not consider past changes in rock properties (i.e. porosity, thermal conductivity), total burial history, and the transient thermal effects from these changes and possible deeper thermal processes such as crustal thinning/thickening and volcanism. Pilaar and Wakefield (1984) used geohistory analysis and the Lopatin method (Lopatin, 1971), correlated to vitrinite reflectance values, to map hydrocarbon kitchens in the Taranaki Basin. They concluded that maturity in the basin decreases from east to west, with the western region being immature probably due to less total sediment thicknesses. They also point out the importance of considering the effective burial time, which plays an important role in source rock maturation because of the time-dependent kinetics involved. In this paper we present a comprehensive re-evaluation of the present-day thermal state of the Taranaki Basin, and use this as the basis for reconstructing complete thermal and oil generation histories for several areas within the basin.

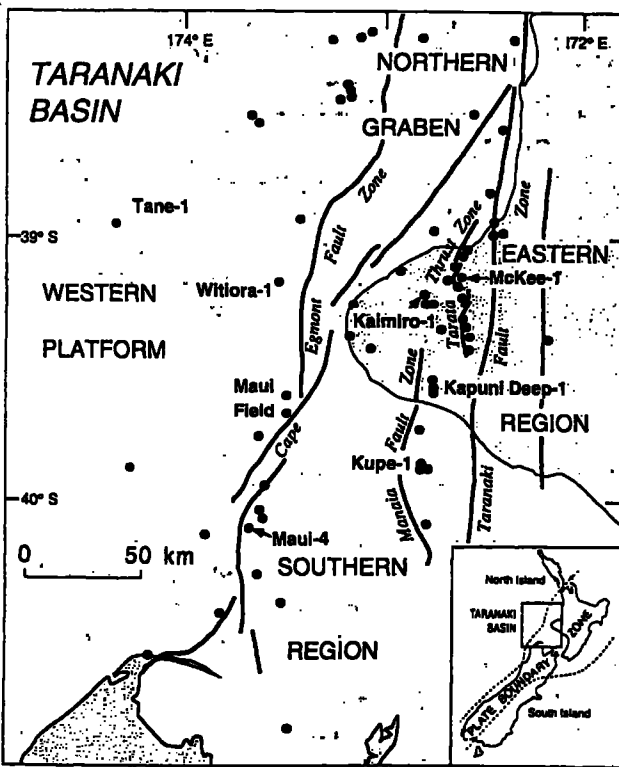


Fig. 1. Location map for the Taranaki Basin showing the main faults and distribution of wells used in the thermal analysis. The named wells are those discussed in the thermal history and hydrocarbon generation section.

## Present-day Thermal Regime

The temperature field in the Taranaki Basin was determined from bottom-hole temperatures (BHTs) obtained from geophysical well-log headers and corrected for thermal effects of drilling (Funnell et al., in prep.). Corrected temperatures from more than 100 wells are shown in figure 3. Present-day temperatures vary from 12–14° C near the surface to about 150° C at 5 km depth. The scatter of temperatures at a common depth in figure 3 is about 35° C, considerably more than the corrected measurement error of 5–10° C, suggesting significant lateral variations exist in the thermal field caused by lithologic, structural, hydrologic, or tectonic processes.

Different symbols in figure 3 denote six geographic regions within the Taranaki Basin. The scatter of corrected BHT data in any one of these groups at depths between 2 and 5 km is less than the spread of all the data, confirming that the overall scatter in figure 3 has in part a geographic origin. The average present-day thermal gradient, assuming a surface temperature of 13° C and a constant gradient with depth, is 29° C/km; local gradients vary from a high value of 32° C/km in the Maui field to about 24° C/km in the southern onshore and Kupe region.

Thermal gradients in sedimentary basins are governed primarily by the thermal conductivity of the sedimentary

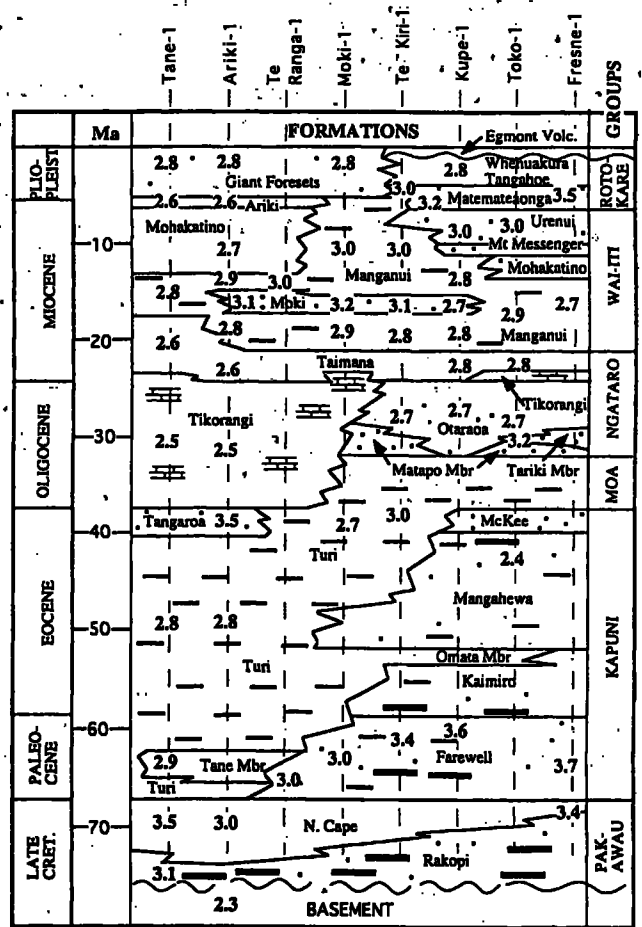
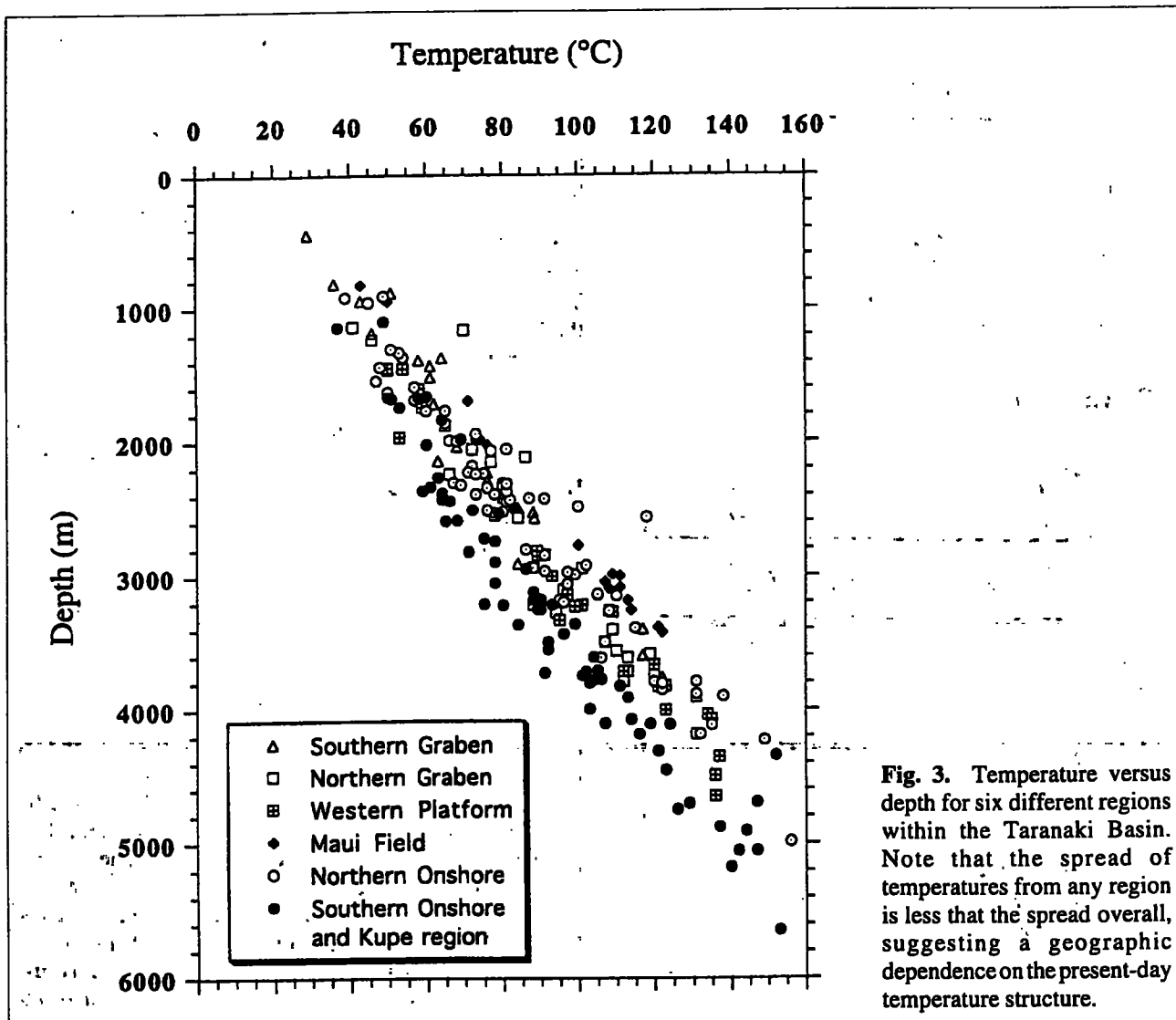


Fig. 2. Generalized stratigraphic section for the Taranaki basin. Bold numbers represent matrix thermal conductivities (in Wm<sup>-1</sup>K<sup>-1</sup>) determined from the lithologic end members for the representative units in the wells listed above the column.



**Fig. 3.** Temperature versus depth for six different regions within the Taranaki Basin. Note that the spread of temperatures from any region is less than the spread overall, suggesting a geographic dependence on the present-day temperature structure.

column and heat flow into the sedimentary section. We have completed 265 thermal conductivity measurements on drill cuttings for eight wells using the cell method described by Sass et al. (1971). The detailed results of the conductivity study are given in Funnell et al., (in prep) and will be described briefly here. In the Taranaki Basin, matrix thermal conductivities vary from  $0.8 \text{ Wm}^{-1}\text{K}^{-1}$  for a coaly shale to  $5.1 \text{ Wm}^{-1}\text{K}^{-1}$  for clean, quartz sandstone. In order to interpolate our laboratory measurements from a 30–70 m sampling interval in eight wells to intervening but unsampled depths in the wells and to extrapolate the results to regions away from the eight wells, we take advantage of a strong dependence of thermal conductivity on lithology. By estimating the lithologic mix of the samples measured in the laboratory we were able to determine the average thermal conductivity of six end-member lithologies: sandstone, siltstone, mudstone, limestone or marl, coal, and andesitic volcanics. A matrix thermal conductivity profile for any well can then be constructed from a lithologic log using an appropriate mixing formula. Representative matrix conductivities for different units in each well that was sampled for conductivity measurements are shown in figure 2. These lithology-derived conductivities are necessary for determining present-day heat flow and also as input parameters for the thermal history and hydrocarbon maturation models.

A porosity-depth relation is used as direct input for correcting thermal conductivity values used in the present-day heat flow and thermal history analyses, as well as to estimate amounts of erosion. Determining porosity-depth relations involves comparing sonic travel times (from sonic logs) with measured porosities (from density logs) where available in the basin. The data in figure 4A are porosity values derived from density logs from the Western Platform region (figure 1). Where no density log porosities are present, porosities can be computed from sonic logs by converting travel times to porosity via the density log porosity-travel time transformation. This method is described and applied to the Beaufort-MacKenzie basin in Canada by Issler (1992) and for the Taranaki Basin by Allis et al. (in prep). The results of the transformation for several wells on the stable Western Platform are shown in figure 4B. The Western Platform has undergone only minor uplift and erosion, if any, thus the porosity-depth relation derived for wells in that area can be used as a datum porosity function. The porosity function for mudstone that best fits the density-log porosity (figure 4A) and the derived sonic-log porosity (figure 4B) for wells on the relatively quiescent Western Platform is

$$\text{porosity} = 54\exp(-z/2000),$$

where porosity is in percent and burial depth ( $z$ ) is in metres. A second, although less robust, porosity function for sandstones and sandy mudstones is

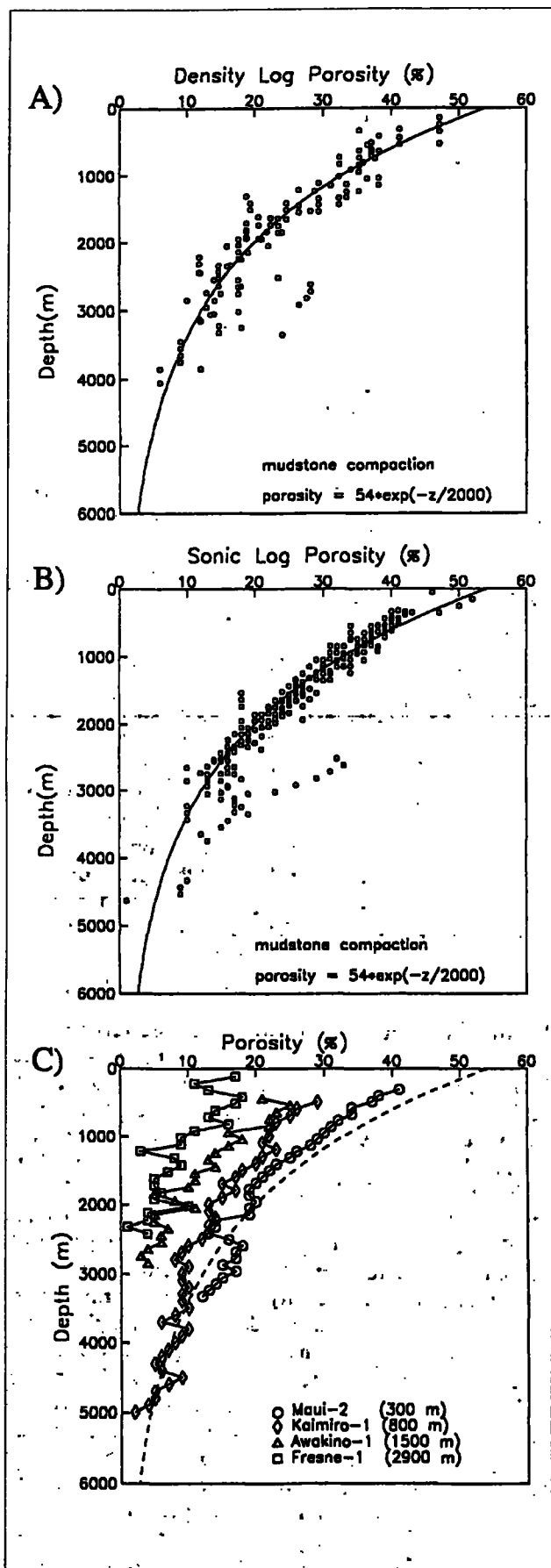


Fig. 4. Porosity versus depth relationships for mudstones used in the thermal analysis. A) Porosity derived from density logs, for wells in the Western Platform region where uplift and erosion has been minimal, assuming a matrix density of  $2.70 \text{ g cm}^{-3}$ . B) Porosity derived from the correlation of density-log porosity with sonic-log travel time. The curve in A and B is the best-fit porosity/depth curve for mudstones. C) Sonic log-derived porosity from four wells illustrating porosity displacement from the datum curve (dashed) derived from the Western Platform wells. The vertical displacement of the porosity curves relative to the datum gives an estimate of the amount of material eroded from the section.

data are from intervals of petroleum interest (reservoir rocks) and not representative of the section as a whole. Deviations from the standard curves are used to determine estimates of erosion (figure 4C). About 2.9 km of erosion (Fresne-1) can be observed in the offset porosity curves for the Taranaki Basin (Allis et al, in prep).

Individual heat flow values for wells in the Taranaki Basin were determined by combining the temperature, conductivity, and porosity information (Funnell et al., in prep). Present-day surface heat flow values are shown in figure 5. The heat flow computation is based on the "Bullard" or thermal resistance method (Bullard, 1939) whereby laboratory thermal conductivity measurements of the rock matrix are converted to porous rock conductivities and corrected for compaction, temperature dependence, and sediment heat production effects (Chapman et al., 1984). The average surface heat flow for the entire basin is about  $60 \text{ mWm}^{-2}$ , not unusual for a basin formed by rifting in the Late Cretaceous. Surface heat flow varies from less than  $50 \text{ mWm}^{-2}$  in the southern Taranaki Peninsula and the Kupe-1 and Toru-1 wells to about  $70 \text{ mWm}^{-2}$  around Cape Farewell in the southern part of the basin and near New Plymouth on the Taranaki Peninsula (figure 5). This spread of present-day surface heat flow values is considerably less than that reported by Pandey (1981) and results primarily from more complete and better calibrated thermal conductivity measurements as well as a more complete BHT dataset. Thermal modelling suggests that the transient thermal effects of erosion and sedimentation, which respectively elevate and depress surface heat flow, are responsible for much of the heat flow variation across the Taranaki Basin. Two additional, and deeper seated processes may also be important. Heat flow may be anomalously depressed to the southeast due to thickening of the lower crust related to deformation caused by the underlying subduction zone, similar to the processes described by Stern et al. (1992). The crustal thickening would produce a heat sink in the lower crust. The high heat flow centred on New Plymouth (figure 5) coincides with the Quaternary volcanic province on the north Taranaki Peninsula, and may be a consequence of mid- or lower-crustal magmatic intrusions.

## Thermal History and Oil Generation Modelling

To simulate the thermal evolution of the Taranaki Basin we used a one-dimensional finite element model (Willett, 1988) that accommodates the conductive thermal effects of variable sedimentation rates, lithologic and depth-dependent thermal

porosity= $45 \cdot \exp(-z/3000)$ .

High-porosity intervals are prevalent in many wells in the basin at depths of 3 to 4 km (figures 4A and 4B) and may represent significant overpressured zones. However, these

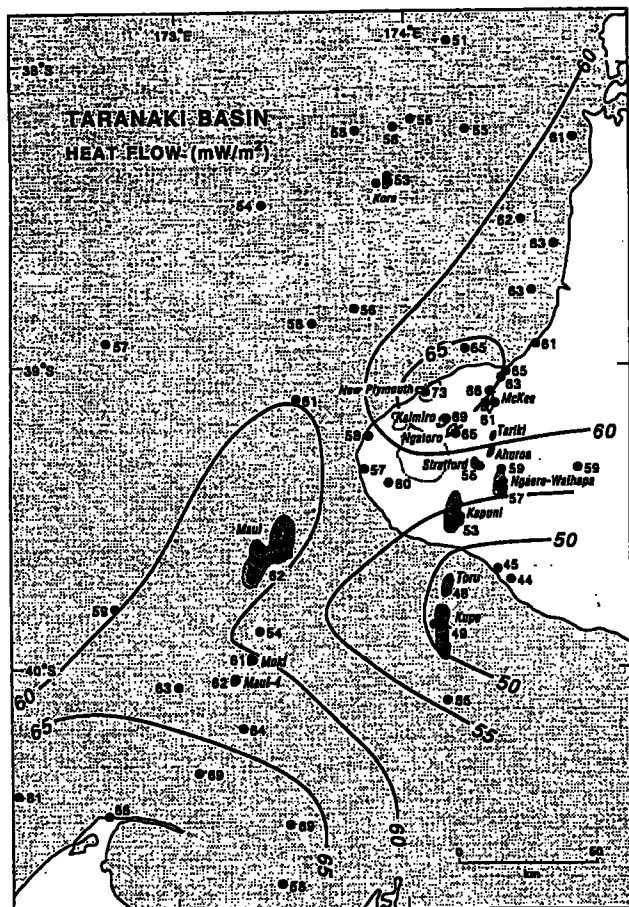


Fig. 5. Present-day surface heat flow trends across the Taranaki Basin (from Funnell et al., in prep.). Contours intervals are  $5 \text{ mWm}^{-2}$ . Note the lateral heat flow gradient of over  $20 \text{ mWm}^{-2}$  across the onshore basin. The dark and light stippled regions represent gas and oil accumulations, respectively. The areas enclosed by dashed lines are volcanic centres.

properties, sediment compaction, syndepositional and synerosional lithospheric thinning or thickening, and instantaneous thrusting.

Model simulations must satisfy both input and output constraints. The input constraints include:

- actual burial history for a specific well
- measured thermal properties of all sedimentary units
- observed porosity/depth functions
- temperature at the top of the sedimentary column (ground surface if subaerial and ocean bottom if subsea)

Present surface temperatures are about  $12\text{--}14^\circ \text{C}$ , and have varied between  $4^\circ \text{C}$  (during deep water periods) and  $20^\circ \text{C}$  for most of the Tertiary. These estimates are based on oxygen isotope and paleontologic evidence for surface water temperatures (Hornibrook, 1992) and temperature versus depth estimates for offshore New Zealand (Ridgway, 1969). This surface temperature variation is as much as  $15^\circ \text{C}$ , depending on age and water depth. It has a significant effect on the subsurface temperatures and leads to large transient thermal signals. The only free parameter in the simulations is the amount of heat flow into the basin (basal heat flow).

The main output constraints of any thermal history simulation are the present-day temperatures (BHTs) in a well. However, BHTs carry no information on the past temperature history of the sediments. Instead, a temperature history can be

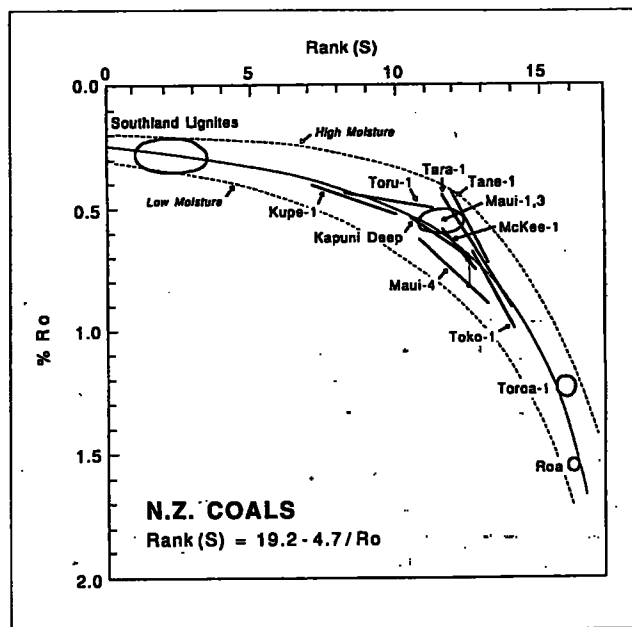


Fig. 6. Coal rank (Rank(S)) versus vitrinite reflectance ( $R_o$ ) for New Zealand coals (derived from Lowery, 1988; Sykes et al., 1992; Suggate and Boudou, 1993; J. Newman, pers. comm.; P. Suggate, pers. comm.). The best-fit curve, shown by the thin solid line given by the inset equation, is used to correct measured vitrinite values if coal rank determinations were made on the same samples (see text). The dashed curves show the effect of moisture on content vitrinite reflectance values, i.e., high moisture content has the effect of decreasing vitrinite reflectance values for any coal rank value (Suggate, 1974).

validated by vitrinite reflectance, coal rank, and apatite fission track ages.

#### Thermal history indicators

The vitrinite reflectance ( $R_o$ ) values listed in Lowery (1988) and Sykes et al. (1992) are used as primary constraints on the thermal history simulations. A related maturation parameter is coal rank (Rank(S) of Suggate, 1959; Suggate and Boudou, 1993) which takes into account coal type as well as moisture and volatile matter content. Rank(S) has been correlated with  $R_o$  for New Zealand coals (figure 6) and an empirical relation has been developed where  $R_o = 4.7/(19.2 - \text{Rank}(S))$ . This curve is fitted to the average  $R_o$  values for each Rank(S) value and allows for the correction of anomalous  $R_o$  values, especially those of coals with high moisture content (which has the effect of lowering  $R_o$ ) to dry, mineral-matter-free values. In wells where both Rank(S) and  $R_o$  values were determined for the same samples, the  $R_o$  values were corrected using the above equation and are noted in the following thermal history simulation discussions. The first-order, Arrhenius reaction kinetic approach of Burnham and Sweeney (1989) was used to produce a  $R_o$  versus depth profile for each thermal history simulation that can be compared with the measured (corrected) data.

Newly acquired apatite fission track (AFT) ages for several Taranaki wells provide further validation of the thermal histories for two wells discussed in this paper. The ages were acquired by the method employed in Kamp and Green (1990) for other wells in the basin. The AFT technique is discussed in several papers (e.g. Gleadow et al., 1986; Duddy et al., 1988; Green et al., 1989a,b; Kamp et al., 1992)

and is not discussed in detail here. In general, this technique can be used to constrain sedimentary basin thermal histories because natural fission tracks in apatite anneal (shorten) at temperatures of 20–130° C over geologic time scales (higher annealing temperatures are possible if heating rates are high) depending on apatite composition. Also, new tracks are progressively added, each with a constant length of about 16 microns resulting in a composite array of tracks with varying lengths. With increasing depth and temperature the tracks anneal, resulting in lower track density and apparent age. Hence, AFT ages are largely a measure of the temperature history of the sample. A second order control on apatite annealing characteristics is composition, namely Cl/(Cl+F) ratios (Green et al., 1986). The forward model of Willett (1992) is used in this study to predict the amount of track annealing and AFT ages of samples with a given thermal history. These modelled results are then compared with measured AFT ages to confirm the thermal history as being acceptable.

### Hydrocarbon generation

Once realistic thermal history models have been determined, the spatial and temporal variations in oil and gas generation can be developed. The qualitative importance of temperature and time to kerogen maturation and oil and gas generation in sedimentary basins has long been recognized (e.g. Waples, 1984). Only recently, however, have the validity and applicability of quantitative models that relate hydrocarbon generation to detailed thermal histories been demonstrated (e.g. Ungerer and Pelet, 1987; Tissot et al., 1987; Quigley et al., 1987; MacKenzie and Quigley, 1988; Wood, 1988; Burnham et al., 1987; Hermanrud et al., 1990; Issler and Snowdon, 1990; Sweeney, 1990; Ungerer et al., 1990; Burrus et al., 1991). These modern approaches to hydrocarbon generation predict amounts, rates, and timing of hydrocarbon generation given a temperature–time path for potential source rock. We incorporated the algorithm of Sweeney (1990) into our basin simulator to solve iteratively at each time step for generation rates and amounts. This method utilises a set of parallel first-order reactions and is based on the Arrhenius equation:

$$dC_i/dt = -A_i C_i \exp(-E_i/RT)$$

where  $C_i$  is concentration of unconverted kerogen,  $E_i$  and  $A_i$  are distributions of activation energies and frequency factors, respectively,  $R$  is the gas constant,  $T$  is absolute temperature, and  $t$  is time.

The source rocks of the Taranaki Basin are typical of high activation energy Type III kerogen. In our simulations of oil generation, the activation energies of Issler and Snowdon (1990) for Type III kerogen are used. Further work in progress to quantify Taranaki kerogen parameters should allow refinement of the generation histories.

For comparison purposes, we consider that appreciable oil generation begins when 10% of the available kerogen is converted to oil. This corresponds to a temperature of about 100° C using the kinetic parameters of Issler and Snowdon (1990) and typical burial histories for Taranaki wells. Although oil is generated at temperatures of about 100° C, its expulsion (liquid phase) occurs at greater depths and temperatures. Cook (1987) suggested that expulsion occurred at  $R_o$  ca. 0.9% which corresponds to depths of 4–5 km in the Taranaki Basin under the present thermal regime. A more recent comparison of biomarker maturity trends of potential

source rocks in the Taranaki Basin, and their apparently related oils, suggests that expulsion occurs at  $R_o$  of 0.8% and Rank(S) of about 13 (Killops et al., in press; Killops et al., this volume) and coincides with a peak hydrogen index of up to 300 (Suggate and Boudou, 1993). These  $R_o$  and Rank(S) values correspond to a potential generation amount of about 30% for the onset of oil expulsion for most source rocks from onshore Taranaki Basin. The 30% generation amount occurs at temperatures of about 130° C for rapid heating rates and less than 120° C for slow heating rates. For discussion purposes, we assume that expulsion begins at 30% generation in all simulations.

### Initial conditions

A basin thermal history simulation is sensitive not only to thermal conditions during sedimentation, but also to the pre-depositional tectonic history of the region. Because time periods are large for conductive thermal processes at lithospheric length scales, rifting, erosion, and crustal melting events that predate basin sedimentation have a long-lived effect on basement heat flow. This changes sediment temperatures for tens of millions of years during the syndepositional history. To show the effects of a pre-depositional history, we consider two end-member initial conditions for the thermal state prior to sedimentation commencing about 75 Ma.

In Case 1, the initial geotherm (at 75 Ma) is based solely on the inferred present-day crustal structure and basement thermal properties and consists of no pre-depositional history. A constant (with time) basal heat flow applied at a depth of 60 km, which results in a minimum least squares error at the end of the simulation between modelled and measured present-day temperatures, is used throughout the entire basin history. The basal heat flow values used are given in Table 1. The pre-depositional (initial) surface heat flow then is the sum of the required basal heat flow for the simulation and the integrated crustal heat production contribution (about 17 mWm<sup>-2</sup>); it is typically 55–65 mWm<sup>-2</sup>.

In Case 2, a pre-depositional tectono-thermal history is considered. It includes a crustal thickening event, mid-lower crustal melting in the overthickened crust, uplift/erosion, and syndepositional rifting as outlined below.

Regional crustal thickening occurred during the Permian to Early Cretaceous along the convergent margin of Gondwana (Coombs et al., 1976; Bradshaw et al., 1980; Mattinson et al., 1986; Tulloch and Kimbrough, 1989). Petrographic and

**Table 1.** Basal heat flow values applied at 60 km depth for Case 1 and Case 2.

Well	Basal Heat Flow (mWm <sup>-2</sup> )	
	Case 1	Case 2
Tane-1	49	34
Witiora-1	49	35
Maui-2	45	30
Maui-4	45	30
Kapuni Deep-1	37	17
Kupe-1	39	19
Kaimiro-1	40	22
McKee-1	40	22

geochemical data from mid Cretaceous Porarari Group granite cobbles suggest that the crust was 45–55 km thick about 112 Ma in SW Nelson region (Tulloch and Palmer, 1990). The Early Cretaceous (114 Ma) Separation Point and Rahu Suite granites, which are the basement rocks for several Taranaki wells, are believed to be derived from melting of overthickened crust, later uplifted and exhumed during extensional collapse and metamorphic core complex development (Kamp and Hegarty, 1989; Tulloch and Kimbrough, 1989). Temperatures required to melt mid crustal rocks (at depths of 20–30 km) are about 600–700° C. To simulate the overthickened crust and granite melt conditions just prior to the onset of uplift and erosion at 120 Ma, we begin Case 2 simulations with a surface heat flow of about 95 mWm<sup>-2</sup> at 120 Ma. Rapid uplift on the scale of 10–20 km occurred between about 120–100 Ma to expose the granites at the surface in the Paparoa region (Tulloch and Kimbrough, 1989). In the Taranaki region, uplifted rocks (Separation Point Granite) were subaerial until deposition of the Late Cretaceous basin deposits occurred, suggesting further erosion. Therefore we consider a modest rapid uplift/erosion of 10 km during the extensional phase (120–100 Ma) followed by a further 2 km of slow erosion (100–75 Ma). At about 75 Ma New Zealand was rifted from Australia during the opening of the Tasman Sea (Weissel and Hayes, 1977). Subsidence analysis based on several Taranaki wells that contain Late Cretaceous sediments suggests a stretching factor of 1.25–2.0. To simulate this rifting event, we incorporate a time-dependent, syndepositional stretching factor of 1.5. The basal heat flow that best satisfies the thermal constraints for each simulation is held constant during the 120 My history. The net effect of this predepositional tectono-thermal history is a surface heat flow of about 90 mWm<sup>-2</sup> at the beginning of Taranaki Basin sedimentation (75 Ma). In Case 2, the required basal heat flow values are lower than in Case 1 (table 1) because the transient effects of the history discussed above cause temperatures to be higher at the start of basin sedimentation, thus allowing the heat input from below to be lower.

Thermal changes due to surface processes affect not only the basin sediments, but the entire lithosphere. Thus, the model lower boundary condition (basal heat flow) must be placed at sufficient depth (60 km) to allow the lithosphere to be affected by transient effects, resulting in longer-lived transient thermal signals. It would be unrealistic to place the lower boundary condition at the base of the basin sediments, because this implies that the basin sediments are decoupled thermally from the basement, which would cause very short transient thermal signals. The constant basal heat flow for both the cases modelled here is an oversimplification and further work on reducing uncertainties in the amounts and temporal changes in basal heat flow is continuing, but since it is applied at lithospheric depths, changes in basal heat flow are not felt in the basin sediments for about 30 My. The most significant changes in the basal heat flow probably occurred about 30 Ma when subduction initiated, but these effects are not yet sensed thermally by the basin sediments. However, subduction-related effects such as lithospheric thickening at depths less than 60 km may perturb the thermal structure in significantly shorter periods of time.

## Site Simulations

Eight of the wells that were analysed for present-day heat flow have been modelled for thermal and oil generation

histories. These include Tane-1, Witiora-1, and Maui-2 wells from the Western Platform region (figure 1); Maui-4 from southern region of the Taranaki Basin; and Kapuni Deep-1, Kupe-1, Kaimiro-1, and McKee-1 from the eastern Taranaki region. These subdivisions are not necessarily based on structural or thermal characteristics, but solely on geographic consideration for discussion purposes. The results of generation and expulsion timing from various stratigraphic horizons, based on the predepositional and generation/expulsion assumptions discussed above, are shown in table 2. The well summary sheets of King (1988) were used to determine depths of horizons and their ages. Isopach and structure contours maps of Thrasher and Cahill (1990) were used to deduce the depths of horizons presently below the maximum depths of penetration in the wells. For each simulation discussed below, we show the modelled temperatures,  $R_o$ , and AFT ages (where available) relative to the measured values. For the modelled present-day temperatures, only Case 1 is shown because Case 2 temperatures are nearly identical. This is an output requirement of the modelling and reflects the thermal properties of both sediments and the observed BHTs. Modelled  $R_o$  and AFT ages are shown for each case if they are different for each case. The depths shown in the geohistories are depths below the top of the sediment column, not below sea level. Thus, changes in water depth are not reflected in the depths of tracked horizons in the geohistories, but they are reflected in depths of isotherms because the temperature at the top of the rock column changes with changes in water depth. Also, it should be noted that the tracked units in the following simulations are not necessarily precise locations of source material, but are reference datums that can be used to interpolate temperatures and hydrocarbon generation amounts for horizons of known source material.

### Western Platform region

It is appropriate to examine the thermal history and hydrocarbon generation first for the Western Platform region because of its relatively simple tectonic history since the Late Cretaceous. Over much of the Western Platform, subsidence has been continuous, although at variable rates, and there has been no significant uplift-erosion.

Subsidence, thermal, oil generation, and generation rate histories for the well Tane-1 are shown in figure 7. Model validation parameters of BHTs,  $R_o$ , and AFT ages are also given. Tane-1 sediments experienced rapid burial between 75–44 Ma, relative quiescence during a passive margin phase until about 15 Ma when deposition recommenced, followed by rapid burial in the last 4 Ma during deposition of the Giant Foresets Formation. Isotherms in the Tane-1 Case 1 geohistory rise (i.e. become shallower) initially due to rapid deposition of high porosity, low conductivity sediments on top of higher conductivity basement rocks, effectively causing temperatures to rise in the basement and offset a general transient cooling that accompanies rapid influx of cold sediments. The rise in isotherms continues after the Late Cretaceous rapid subsidence phase as the lithosphere recovers towards thermal equilibrium. At 28 Ma there is a sharp depression in the isotherms due to increased water depth accompanying rapid subsidence and a corresponding decrease in water bottom temperature. This isotherm depression at 30–20 Ma is typical of most of the following simulations and is probably associated with platform subsidence during the first stages of convergent

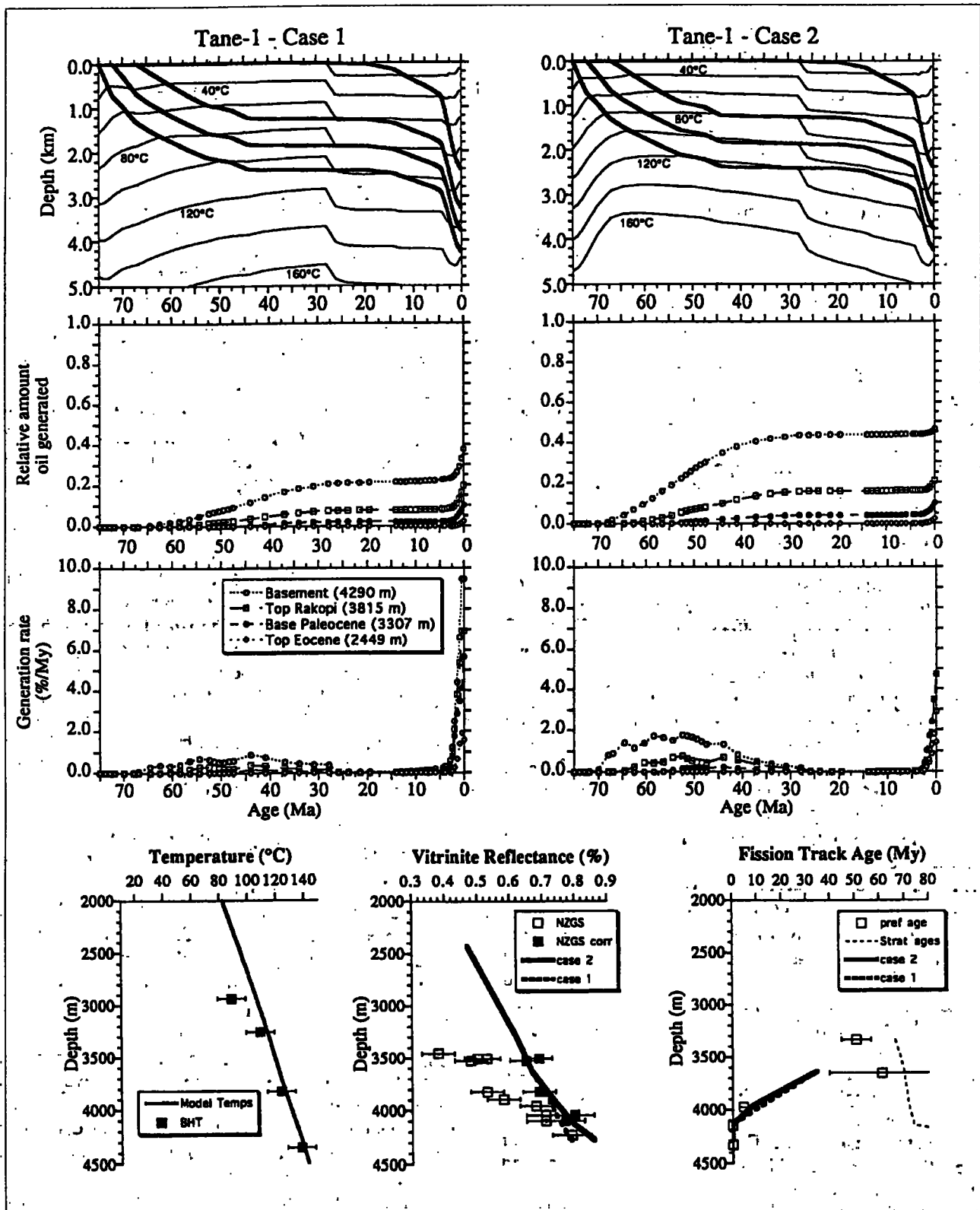


**Fig. 7.** Geohistory, relative oil generation amounts, and generation rates for Tane-1. Case 1 and Case 2 represent low heat flow and high heat flow initial conditions, respectively. Case 2 simulations were run from 120 Ma, but only the last 75 My of the simulations are shown here. See text for discussion. The tracked units (bold lines) in the geohistory plots correspond to the horizons and depths (present day) given in the generation rate plot insets. The thin lines in the geohistory plots are isotherms in 20° C intervals. 'Relative amounts oil generated' refers to the total relative mass of available kerogen converted to oil, i.e. 1.0 is 100% of kerogen converted. Plots at bottom are depth profiles of modelled and measured temperature, vitrinite reflectance, and apatite fission track ages (where available). Bottom hole temperature errors are  $\pm 10^{\circ}$  C and the vitrinite reflectance and fission track age errors are  $\pm$  one standard deviation. The 'NZGS corr.' data in the vitrinite reflectance plot are the Rank(S)-corrected vitrinite reflectance values (see figure 6). 'pref age' refers to preferred fission track age and 'strat age' to age of strata sampled for AFT age determination. NZGS is New Zealand Geological Survey. All depths are relative to the top of the rock column.

margin tectonics between 30–25 Ma (Holt and Stern, in press).

The Case 2 simulation for Tane-1 has a more pronounced rise in the isotherms between 75 and 65 Ma due to the combination of low conductivity sediments and the transient thermal effect of syndepositional rifting. Isotherms have a maximum elevation about 65 Ma and decay downward to the present-day. Heat flow in Case 2 was higher than in Case 1 by about 30% after the initial rapid subsidence; this is a long-lived thermal signal that particularly affects the deeper horizons in Tane-1 (Basement and Top Rakopi horizons in figure 7) until the depression of isotherms occurs associated with rapid deposition in the Plio–Pleistocene. The initial rise in the isotherms is typical of all the wells discussed, but in varying amounts depending on sedimentation rate.

In both cases the relative amount of oil generated at Tane-1 is 40–45% of kerogen volume for deepest Pakawau Group rocks at the basement horizon, and about 20% for Top Rakopi. For Case 1, the entire Rakopi section is presently at its maximum generation rate. In Case 2 the deepest Rakopi sediments ('Basement' horizon) presently have a maximum generation rate as well (about 3% per My), but during the Paleogene the rates were also relatively high at about 2% per My.

Tane-1 source rocks are considered to be immature, yet the generation plots (figure 7) suggest that appreciable generation could have occurred in suitable source rocks since about 61 Ma for the basement horizon with expulsion as early as 48 Ma at temperatures of about 120° C for Case 2 (table 2). Therefore, if sufficient source rocks in the area were at depths the same as the deepest Rakopi section in Tane-1, significant oil may have been generated and expelled in the Eocene or later.

Modelled and measured temperatures,  $R_o$ , and AFT ages are shown at the bottom of figure 7. Both Case 1 and Case 2 simulations provide acceptable fits to the observational constraints, but corrected  $R_o$  values and AFT ages require model temperatures at the high end of the acceptable range of BHT data. The dashed and solid curves on the  $R_o$  and AFT age plots represent Case 1 and Case 2, respectively, and show that  $R_o$  and AFT ages are relatively insensitive to the early higher heat flow of Case 2 because they are mostly sensitive to the maximum temperatures, which were achieved in both cases near the end of the thermal history. The shallowest samples have AFT ages that are close to stratigraphic ages indicating that they probably contain a large component of inherited tracks from the provenance terrane (Kamp and Green, 1990). This is typical of samples from several Taranaki wells.

We have modelled (but do not illustrate) two further wells in the Western Platform region, Witiara-1 and Maui-2. Hydrocarbon generation and expulsion timing is given in table 2. Witiara-1, like Tane-1, experienced rapid Plio–Pleistocene subsidence that controls temperatures and oil generation. The relative generation amount of 10% occurred in the last 5 My for Case 1, but as long ago as 28 Ma for Case 2, yet expulsion has occurred only in the last 1 My, if at all, for the deepest potential source rocks (Paleocene–Eocene) (table 2). The entire Eocene section however has reached oil generation depths in Witiara-1, whereas the same section in Tane-1 is too shallow for significant oil generation.

In Maui-2 (and the Maui Field in general), the deepest sediments reached their maximum temperature of 111° C in the last 2 My; they have been immature since deposition. Even though this region is immature, it is the location of major gas/condensate and associated oil accumulations, indicating migration of the hydrocarbons from other sources. It has been suggested that hydrocarbons in the Maui structure migrated either up the Cape Egmont Fault located to the east or from the north and along the Cape Egmont Fault zone since reactivation of the fault in a normal sense during the Plio–Pleistocene (Haskell, 1991). Recent work on helium isotopes from Maui gases suggests an interaction with magmatic gases (Giggenbach, 1993); the only known source or recent volcanic activity is located about 50 km northeast of the Maui Field. This suggests that some component of the Maui gases might be derived from a northern source. Killops et al. (this volume) suggest that a mantle gas signature may be due to seepage of gas through crustal-scale fractures identified in the North Taranaki Graben and along the Cape Egmont Fault Zone (figure 1). Thrasher (1990b) speculated that migration of hydrocarbons may have been possible in the late Miocene prior to reactivation of the Cape Egmont Fault Zone. Thermal modelling of this region (just east of the Cape Egmont Fault Zone) suggests that maximum generation within the Late Cretaceous coal measures of Rakopi Formation were generating oil at rates of 4–5% per My during the late Miocene and rates as high as 6% per My in the Plio–Pleistocene with 30% of available kerogen converted prior to 10 Ma. Thus it is possible that hydrocarbons may have been generated early (Miocene) and migrated to present positions during the most recent movement of the Cape Egmont Fault Zone, and prior to the Plio–Pleistocene phase of hydrocarbon generation.

#### Southern Taranaki region

The southern Taranaki region is part of the Southern Inversion Zone (King, this volume) and has undergone a more complex tectonic history than the Western Platform region. Both regions experienced the same Late Cretaceous rift, subsidence, and early Tertiary passive margin phase, but the Southern Inversion Zone was subjected to late Miocene uplift during convergent margin tectonics and later reactivation of several reverse faults into normal faults during Plio–Pleistocene subsidence. An example of the thermal history and hydrocarbon generation is shown in figure 8 for Maui-4. The site experienced initial rapid subsidence, passive margin phase, and rapid subsidence/deposition at about 25 Ma, similar to that discussed previously for Tane-1. Maui-4 area then experienced rapid uplift about 6 Ma followed by subsidence in the last 4 My.

Regardless of a hot (Case 2) or cool (Case 1) start, the oil generation rate for the Late Cretaceous section ('Basement' to 'Base Farewell' in figure 8) was at a maximum between about 10–6 Ma. Case 2 shows that significant generation in the Rakopi section, which contains coal measures that show the best correlation with Maui-4 oils (Killops et al., this volume), may have occurred as early as 62 Ma, but sufficient maturity for expulsion, based on 30% generation, was not reached until about 10 Ma for Case 1 and 38 Ma for Case 2 (table 2). In Case 2, the early expulsion from the deepest Rakopi potential source rocks would have occurred at temperatures as low as 115° C, illustrating the effect of slow heating rates on oil generation and expulsion. In both cases, generation rates decreased to zero for the entire sedimentary

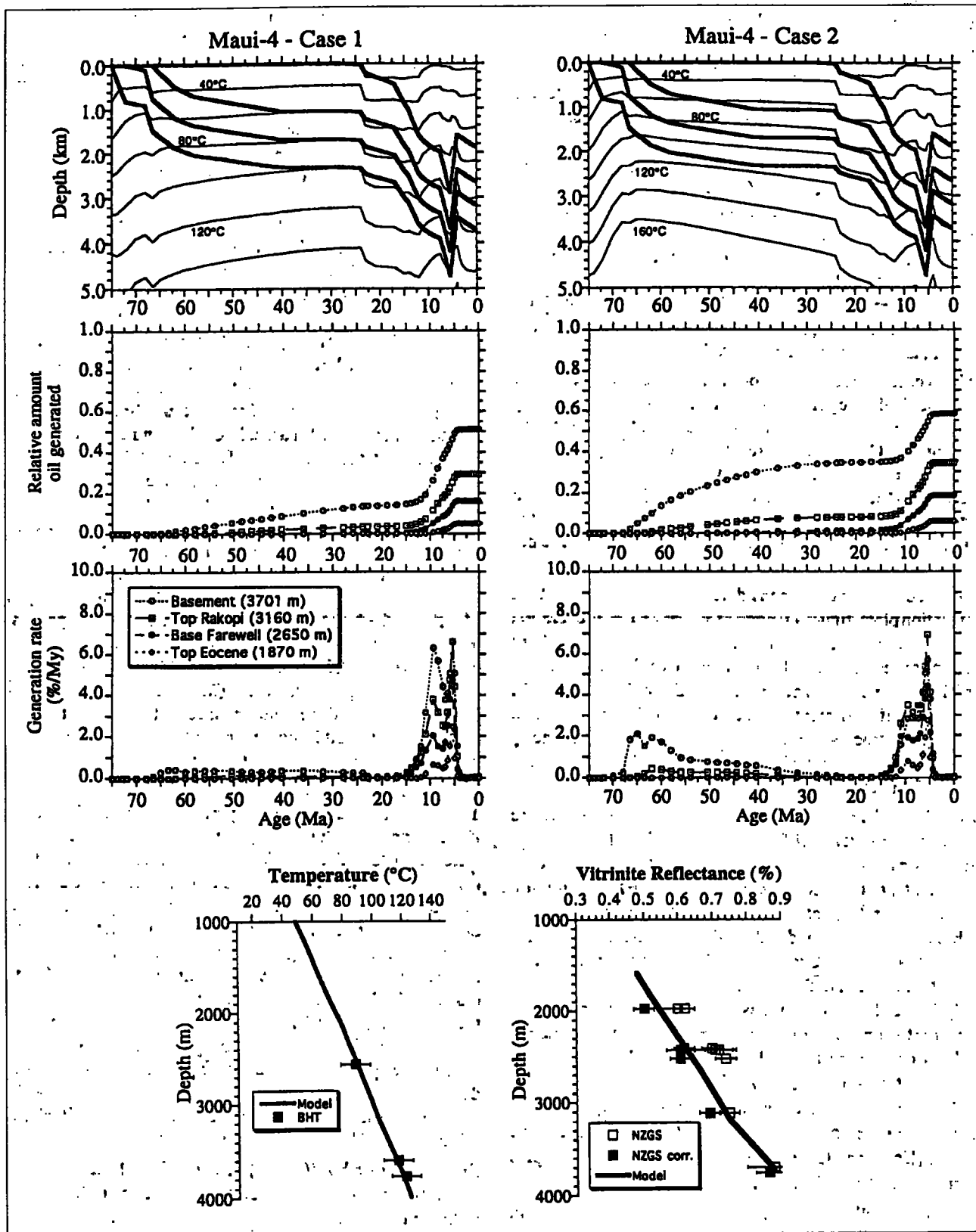


Fig. 8. Geohistory, relative oil generation amounts, and generation rates for Maui-4. See figure 7 for further description of plots.

section about 5 Ma, immediately after the late Miocene uplift phase. The Maui-4 region presently is not generating hydrocarbons. An organic biomarker study of Maui-4 oils and coals (Johnston et al., 1988) indicates that sufficient maturity would be expected in the Maui-4 region at depths of about 4000 m (presently below basement). This is consistent with the present-day thermal regime. It appears, however, that appreciable generation may have occurred in

the late Miocene, prior to about 1300 m uplift and erosion (Allis et al., in prep), with migration at that time out of the Maui-4 region and into other immature regions such as the Maui Field or other undiscovered reservoirs.

#### Eastern Taranaki region

The eastern Taranaki region displays the same general Late Cretaceous rift episode, passive margin phase, and late Oligocene subsidence as both the Western Platform and

southern Taranaki regions. Miocene subduction-related compression caused deformation associated with the Taranaki, Manaia, and Tarata Thrust zones (figure 1). This was followed by Miocene–Pliocene subsidence and then, in the last 2 My, varying amounts of uplift and erosion. These histories are illustrated in the geohistory plots in figures 9–11. Figure 9 shows the Case 1 and Case 2 geohistories and oil generation histories for Kapuni Deep-1. Basement and Top Rakopi Formation horizons show that initial rapid subsidence

lasted for about 18 My during which as much as 5 km of Late Cretaceous–Paleocene sediments were deposited. Slower subsidence continued until the late Miocene when a 300 m erosion event occurred. Structural cross-sections (King et al., 1991) show a reverse fault (the Manaia Fault) just west of the location of the Kapuni and Kupe fields (figure 1) with up to 2000 m of stratigraphic separation. Even though this fault probably was accumulating displacement between the early and late Miocene, the entire area was experiencing

**Table 2.** Onset of oil generation and expulsion and the maximum temperature reached by each tracked unit in thermal history simulations. Oil generation is assumed to begin when 10% of available kerogen is converted to oil and corresponds to  $R_o$  of 0.6, Rank(S) of 11.5, and a temperature of about 100° C at typical heating rates. Expulsion is assumed to begin at 30% of the kerogen converted to oil and corresponds to  $R_o$  of 0.8, Rank(S) of 13.0, and a temperature of about 130° C at typical heating rates.

Well	Unit	Present Depth (m)	CASE 1			CASE 2		
			Oil Gen. (Ma)	Expul. (Ma)	Max. Temp (°C)	Oil Gen. (Ma)	Expul. (Ma)	Max. Temp (°C)
<b>WESTERN PLATFORM</b>								
Tane-1	Basement	4290	47	1	138	61	48	138
	Top Rakopi	3815	2	-	125	44	-	125
	Base Paleocene	3307	-	-	109	-	-	109
	Top Eocene	2449	-	-	89	-	-	89
Witiora-1	Basement	4070	5	1	130	28	1	130
	Top Eocene	2915	-	-	104	-	-	104
Maui-2	Basement	3338	2	-	111	2	-	111
	Base Mangahewa	3124	1	-	107	1	-	107
	Top Eocene	2566	-	-	92	-	-	92
<b>SOUTHERN REGION</b>								
Maui-4	Basement	3701	36	10	143	62	38	143
	Top Rakopi	3160	10	6	131	11	7	131
	Base Farewell	2650	7	-	118	7	-	118
	Top Eocene	1870	-	-	102	-	-	102
<b>EASTERN TARANAKI REGION</b>								
Kapuni Deep-1	Top Rakopi	7600	60	53	162	67	65	162
	Base Farewell	5800	37	17	140	58	42	140
	Base Kaimiro	3988	2	-	108	2	-	108
	Base Mangahewa	3600	0.1	-	102	0.1	-	102
Kupe-1	Basement	6260	62	42	135	68	66	135
	Top Rakopi	5260	27	-	122	62	44	122
	Top North Cape	3960	-	-	102	-	-	102
	Top Farewell	3170	-	-	86	-	-	86
Kaimiro-1	Basement	5696	30	10	155	45	18	155
	Top Rakopi	5546	21	9	152	38	13	152
	Base Mangahewa	4295	8	4	133	8	5	133
	Top Eocene	3490	5	-	119	5	-	119
McKee-1	Basement	6800	57	40	180	69	64	180
	Top Rakopi	5744	34	12	161	48	12	161
	Base Paleocene	5000	13	8	150	26	10	150
	FW-Top Eocene	3475	6	-	121	7	-	121
	HW-Top Eocene	2390	-	-	100	-	-	100

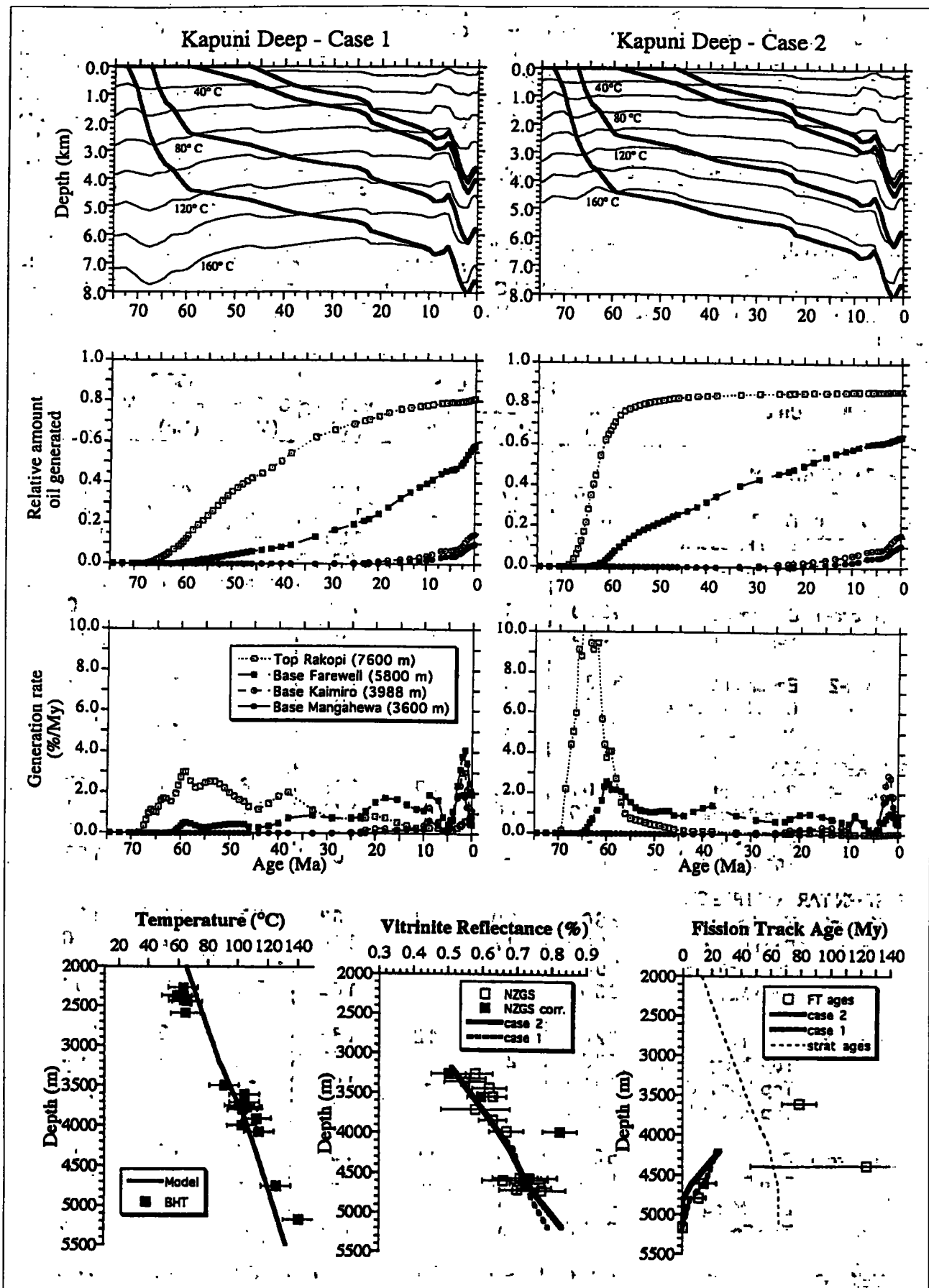


Fig. 9. Geohistory, relative oil generation amounts, and generation rates for Kapuni Deep-1. - See figure 7 for further description of plots.

regional subsidence, probably related to foreland loading farther east (Holt and Stern, in press), and deposition on top of the growing structure. Hence, because the geohistory curves show depth from top of the sediment column, they do not reflect this 'apparent uplift' event until the late Miocene

when about 300 m was eroded. This is followed by Pliocene rapid subsidence and finally about 500 m of Pleistocene uplift.

In Case 1, oil generation in Kapuni Deep-1 area would have begun about 60 Ma for the deepest inferred source rocks

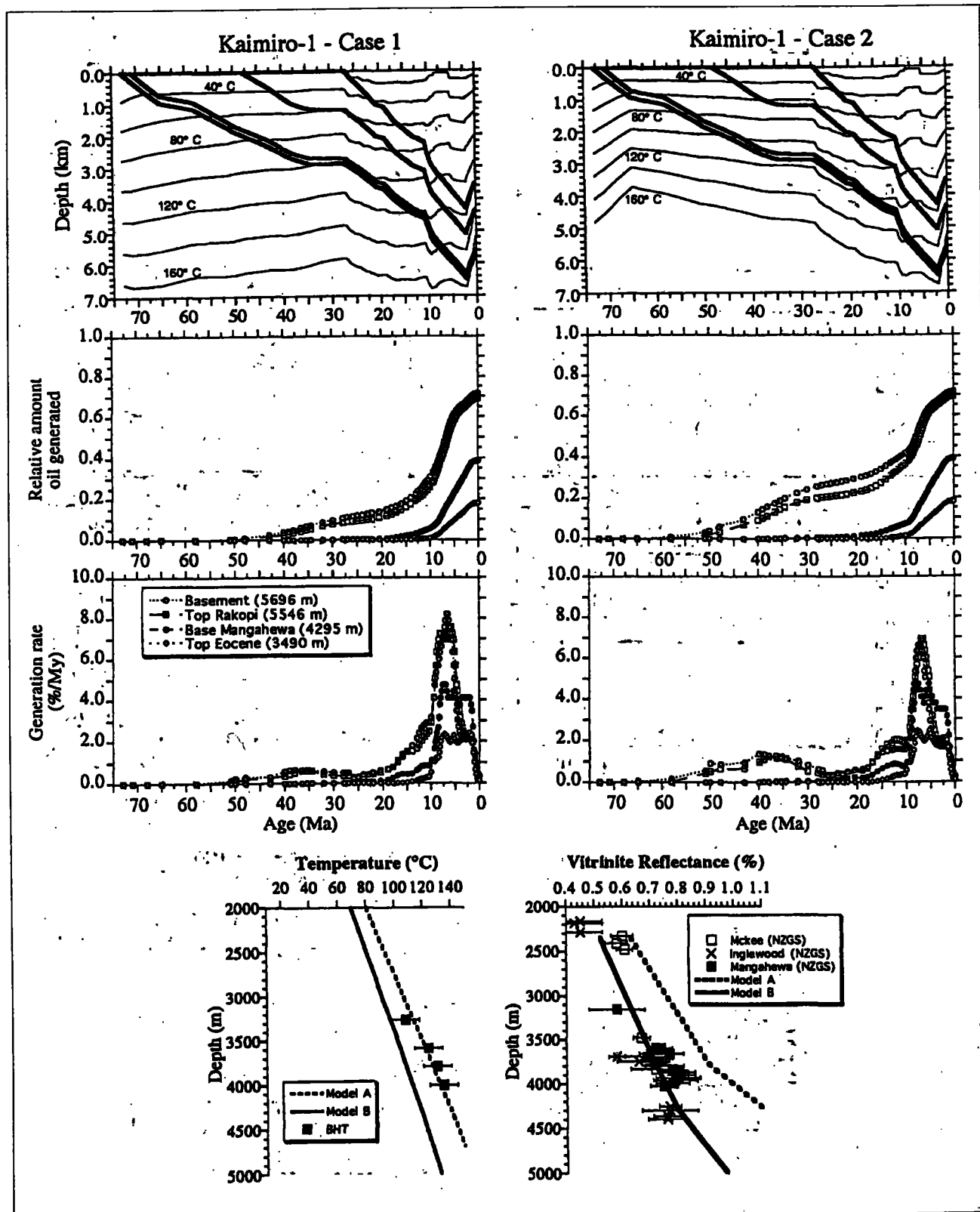


Fig. 10. Geohistory, relative oil generation amounts, and generation rates for Kaimiro-1. In the temperature and vitrinite reflectance plots, Model A reflects high heat flow in the Quaternary in order to satisfy the present-day temperatures and Model B reflects the pre-Quaternary lower heat flow that better satisfies the vitrinite reflectance and Cenozoic heat flow of nearby wells (see text). Note that the higher heat flow in Model A causes severe overestimation of vitrinite reflectance. See figure 7 for further description of plots.

(below 'Top Rakopi' in figure 9 and table 2). For Case 2 these units would have generated oil even earlier because of the rapid deep burial and high initial heat flow. In fact, the generation amount plots for Case 2 (figure 9) show that

almost all (about 85%) the predicted oil generation and expulsion would have occurred between about 65 and 55 Ma, when the generation rates reached values of greater than 10% per My, with little or no generation since then. In

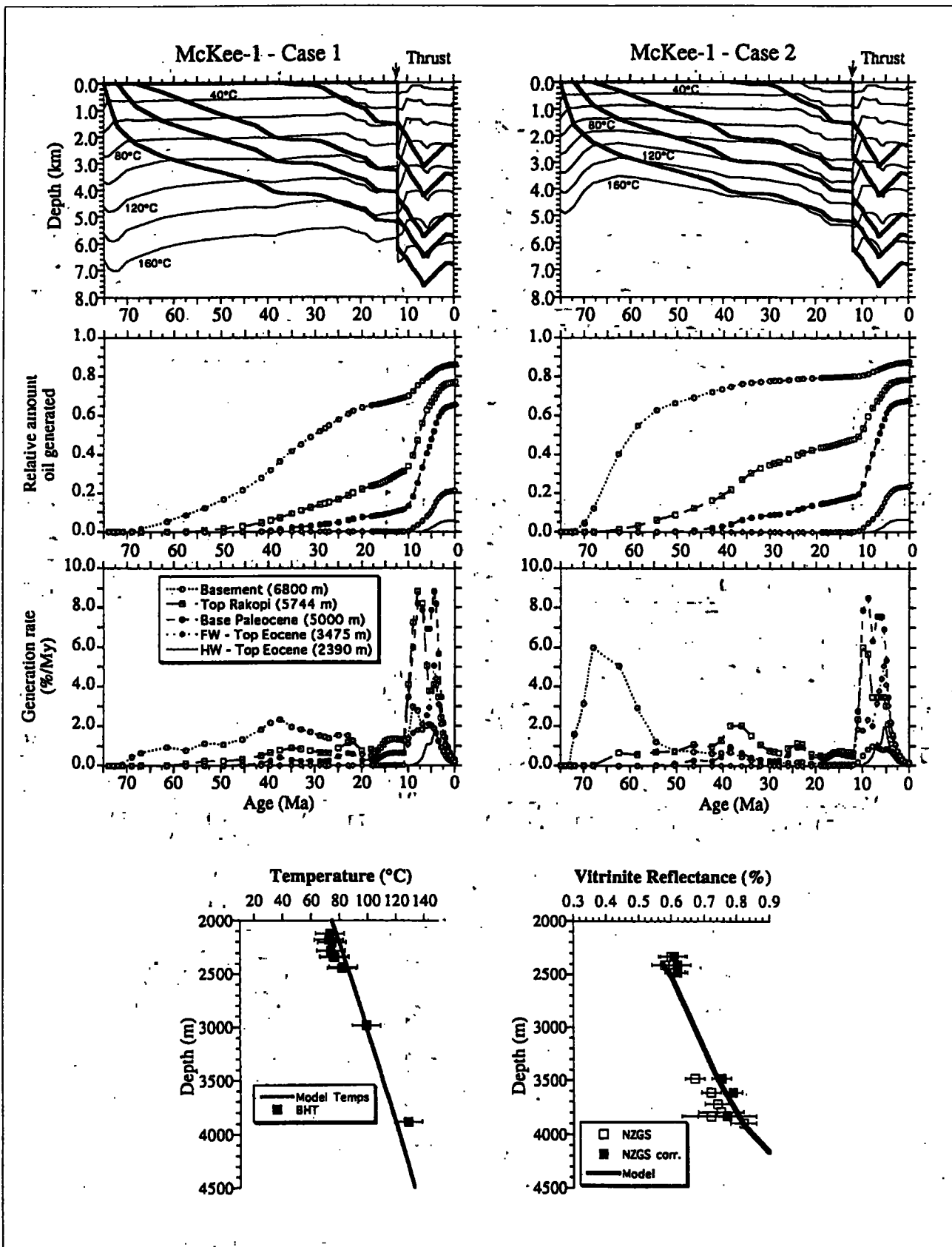


Fig. 11. Geohistory, relative oil generation amounts, and generation rates for McKee-1. 'Thrust' refers to the Tarata Thrust (figure 1). The instantaneous depth increase for all the tracked units reflects the instantaneous emplacement of the Tarata Thrust, assuming a hanging wall overthrust thickness of 1.5 km. The shallowest tracked horizon is the top of the Eocene section in the overthrust sheet (see text for details). See figure 7 for further description of plots.

Case 1, almost as much of the generative potential has been realised (about 80%), but generation was continuous with at least some oil generated in the Rakopi section during the entire Tertiary subsidence history. Although the Case 2 example predicts earlier Rakopi generation and expulsion and probably very early migration from the source region, both cases show that possible Rakopi strata below Kapuni Deep-1 are presently at temperatures of 160–170°C and out of the oil window. It may be generating and expelling gas today from preserved kerogen or cracking from oil if the oils were trapped and are still present in the area.

Killops et al. (this volume) show that biomarker distributions of oils and condensates in the Kapuni Field are consistent with Paleocene sources. The bottom of the Paleocene section ('Base Farewell' in figure 9) is currently at a temperature of about 140°C, with the section of the Farewell Formation below about 5300 m at sufficient temperatures for expulsion (about 130°C). This is shallower than the present-day depth of 6000 m or more for Kapuni Field oil expulsion predicted by Johnston et al. (1990), but is close to the present-day depth estimate of 5500 m for oil expulsion of Killops et al. (this volume). The inferred base of the Farewell Formation has generated 60–65% of hydrocarbons from available kerogen (figure 9). Even though parts of the Farewell Formation may presently be generating and expelling hydrocarbons, the beginning of generation and expulsion was earlier, with significant differences between the initial condition cases. In Case 1, generation began about 37 Ma and expulsion about 17 Ma, whereas in Case 2, the timing is 58 Ma and 42 Ma, respectively. Therefore, the bottom of the Farewell section may have been expelling hydrocarbons as early as the latest Eocene, prior to the initial stages of reverse faulting along the Manaia Fault.

The Eocene section in Kapuni Deep-1, which includes the Kaimiro and Mangahewa formations, is currently immature. Maximum generation rates for the base of the Eocene section ('Base Kaimiro' in figure 9) were about 3% per My about 2 Ma when temperatures reached a maximum of 108°C, prior to 500 m of Quaternary erosion. The generation plots (figure 9) show that only about 15% or less of available Eocene kerogen would have been converted to hydrocarbons in the Kapuni Field.

The modelled temperatures,  $R_o$ , and AFT ages are shown at the bottom of figure 9. Both Case 1 and Case 2 give acceptable fits to the  $R_o$  and AFT data, although there is a slightly better fit in Case 1 for the modelled AFT ages. The shallower samples have ages that are older than stratigraphic ages and probably reflect a provenance age. The model temperature profile matches average BHT values, but systematically overestimates BHTs at 2500 m depth and underestimates the deepest observations.

The geohistory for the Kupe-1 area is similar to that of Kapuni Deep-1, and is discussed only briefly here. The Kupe-1 and Kapuni Deep-1 sites have similar present-day surface heat flow values of 49 and 53 mWm<sup>-2</sup>, respectively (figure 5). The principal difference in the Kupe-1 and Kapuni Deep-1 burial histories is that Late Cretaceous sediments below Kupe-1 were not buried as deep prior to late Miocene rapid subsidence. Thus the 'Top Rakopi' is about 2 km deeper below Kapuni Deep-1 than below Kupe-1.

For both Case 1 and Case 2 in Kupe-1, oil generation began in the Paleocene for the deepest basin sediments (Rakopi

Fm). Expulsion in this unit began about 42 Ma for Case 1 and 66 Ma for Case 2 (table 2). Thus, if a Case 2 scenario is considered, the base of the Rakopi section below Kupe-1 had very early expulsion and migration. For Case 1, expulsion and migration from most of the Rakopi section would have occurred mostly since the Miocene and this oil may have migrated into Miocene contractional structures. This same section in Kapuni Deep-1 is considered to have been overmature at least since the Miocene. In Kupe-1, the Paleocene section has never been at sufficient oil generation temperatures and less than 10% of the generative potential has been realised. However, in Kapuni Deep-1, this section is considered the main source for oils and condensates (Killops et al., this volume) and is currently, at least partly, in the oil window.

Kaimiro-1 has a present-day heat flow of 69 mWm<sup>-2</sup> and is adjacent to a heat-flow high centred on New Plymouth. This heat-flow high for the northern Taranaki Peninsula is 35% higher than the heat flow values of the southern Taranaki Peninsula (compare New Plymouth with Kapuni in figure 5), and has significant consequences in terms of the timing of oil generation in the eastern Taranaki basin region.

In order to fit the measured BHTs, the required basal heat flow values are 53 mWm<sup>-2</sup> and 38 mWm<sup>-2</sup> for Case 1 and Case 2, respectively. However, basal heat flow values of about 44 mWm<sup>-2</sup> (Case 1) and 22 mWm<sup>-2</sup> (Case 2) are required to match the  $R_o$  data from wells near Kaimiro (there are no reliable  $R_o$  data from Kaimiro or New Plymouth). We chose the lower set of basal heat flow values for Kaimiro (table 2) and interpret them to be more characteristic of this part of the basin for most of its history; the lower basal heat flow values are the same as those required by nearby McKee-1. The higher present-day temperatures may be due to nearby Quaternary volcanic activity (Funnell et al., in prep). Therefore, the modelled temperatures (Model A) in the temperature versus depth profile at the bottom of figure 10 reflect the higher heat flow applied late in the history, whereas the modelled  $R_o$  values and oil generation histories reflect the lower heat flow (Model B). Presumably, reliable  $R_o$  values from wells in the high heat flow region would match those predicted by Model A, with the high values probably being reached in the last 2 My.

Tracked horizons in Kaimiro-1 display roughly linear subsidence trends in the geohistory plots of Figure 10 between 72 and about 2 Ma. This results in the Rakopi section being at shallower depths early in its history when compared to Kapuni Deep-1. Below Kapuni Deep-1 the 'Top Rakopi' reaches 4 km depth by about 60 Ma, but the same depth is reached about 17 Ma below Kaimiro-1. The top of the Rakopi section, therefore, probably did not begin oil generation until 21 Ma for Case 1 and 38 Ma for Case 2; this is 35 My later than Rakopi oil generation below Kapuni Deep-1. Expulsion from the Rakopi began about 10 Ma below Kaimiro-1 for both cases and the oil may have migrated into contractional structures formed previously in the region or into Manaia structures in the Kapuni area to the south which were forming at that time.

Maximum generation rates for the Late Cretaceous through Eocene source rocks in Kaimiro-1 occurred between about 10 and 2 Ma, prior to 1000 m of Quaternary uplift. During the uplift, generation rates decreased rapidly (figure 10). However, with the inferred Quaternary temperature increase,

the generation rates for each unit would be higher in the last 2 My than shown in figure 10, with generation probably occurring today out of most of the Late Cretaceous through Eocene sequence. The Eocene section in Kapuni Deep-1 is considered to be immature (see discussion of Kapuni Deep-1), whereas in the Kaimiro region Eocene source rocks probably were expelling oil by about 5 Ma. This reflects the greater burial depths of the source rock section (compare 'Base Mangahewa' in figures 9 and 10 and table 2) prior to Quaternary uplift.

The McKee Field lies within the Miocene Tarata Thrust zone (figure 1) and contains economical oil deposits in reservoirs within the McKee Formation in the hanging wall of the thrust. The geohistories and generation histories for the McKee-1 site are shown in figure 11. The McKee-1 site shows rapid initial subsidence followed by roughly linear subsidence starting about 65 Ma. Cross-sections across the Tarata Thrust (King et al., 1991) indicate that early Southland Series strata are cut by the thrust and are relatively thin in the hanging wall suggesting a Southland age (10-16 Ma) for thrusting. We simulate this relatively rapid thrust event with instantaneous thrusting at 12 Ma. This is shown by the increase in depths of all tracked units in the geohistory plots of figure 11. The uppermost tracked horizon is the top of the Eocene section in the hanging wall of the thrust. Since the geohistory plots represent emplacement ages of the rocks relative to the footwall block, the hanging wall Eocene section appears at 12 Ma, the age that it was emplaced above the footwall. The instantaneous depression of the isotherms, relative to the top of the overthrust section, at 12 Ma is the result of footwall rocks instantaneously being 1.5 km deeper after thrust emplacement. The isotherms rapidly re-equilibrate as the footwall rocks are heated at the new depths.

In Case 1, the base of the Rakopi Formation ('Basement' in figure 11) below McKee-1 generated oil about 57 Ma, with expulsion as early as 40 Ma. The top of the Rakopi began generating 34 Ma but did not begin expulsion until the overthrust section was emplaced. For Case 2, generation and expulsion for the base of the Rakopi were earlier (table 2), with possible expulsion as early as 64 Ma. It is possible, therefore, that at least parts of the Rakopi Formation were within the expulsion window from 64 Ma to just after thrusting, when temperatures exceeding the oil generation window were reached. Temperatures are presently 155-175° C in the Rakopi Formation below McKee-1.

Killops et al. (this volume) suggest the oils in the McKee Field are sourced predominantly by Eocene coals perhaps from areas east of and down-dip (in the overthrust section) from the McKee Field. For the top of the footwall Eocene section in figure 11, maximum generation rates occurred about 5 Ma, regardless of which initial case is considered, coincident with maximum burial of 4.2 km. Ten percent of the potential generation occurred 6-7 Ma, but sufficient maturation for expulsion never occurred at the top of the Eocene section, confirming the conclusion that the McKee oils were probably derived from farther east. The base of the Paleocene (figure 11) also had maximum generation rate between 12 and 5 Ma, but expulsion occurred at 10 Ma, just after thrusting. Therefore, at least some of the Paleocene section was expelling oil in the last 10 My. Maturation of the Paleocene section in McKee-1, due predominantly to the increase in burial depth during thrusting, occurred a few million years prior to equivalent maturation in Kaimiro-1

(table 2). McKee-1 generation rates, as in Kaimiro-1, decreased during Pliocene and Quaternary uplift but temperatures in the Paleocene section are presently high enough for expulsion in both areas. The oil generated in the Paleocene-Eocene section below the thrust of McKee-1 probably was expelled westward toward the Kaimiro region and may have been a contributor to the oil found in reservoirs within the Miocene Mt Messenger Formation in that area.

## Summary

Thermal history modelling provides the link between observations such as basin temperatures, porosity, thermal conductivity, and deposition-erosion history and the amounts and rates of hydrocarbon generation. The thermal histories are validated as being acceptable models, although not necessarily unique, by thermal history indicators such as vitrinite reflectance, coal rank, and apatite fission track ages.

In this study we have constructed the thermal and generation histories, based on the above observations, for three regions of the Taranaki Basin. Two end-member initial condition scenarios were considered: one in which a subjective initial heat flow is assumed, and another that incorporates predepositional Mesozoic tectono-thermal events (crustal thickening and rifting) that results in higher heat flow initially. Thermal history indicators in the Taranaki Basin, however, cannot discriminate between these two models because the vitrinite reflectance and apatite fission track ages are insensitive to the early thermal state and record mostly the maximum temperatures, which were reached long after basin initiation. Therefore, at this stage the thermal histories and timing of modelled oil generation, particularly prior to the Miocene, are equivocal. The two cases presented in this paper probably represent end-member scenarios of the possible thermal and oil generation histories. Better defining of the initial conditions and basal heat flow histories and their effects on oil generation is the subject of ongoing research.

In the Western Platform region, temperatures are currently at a maximum mainly due to continuous subsidence (though not at a uniform rate) and lack of uplift/erosion. In this region, potential source strata are considered relatively immature with generation amounts sufficient for expulsion in Tane-1 and Witiara-1 areas being reached only in the last one million years for most of the Rakopi section, but possibly as early as the Eocene for the deepest Rakopi rocks.

In the southern Taranaki region, the thermal and oil generation histories of the Maui-4 site were assessed. The potential source strata (Rakopi Formation) are presently at temperatures of less than 120° C. However, they reached temperatures of up to 140° C and had maximum generation rates in the late Miocene prior to uplift and erosion. Any hydrocarbon generated and expelled at that time probably migrated to other areas or was lost from the system. At least parts of the Rakopi source rock section may have been expelling oil as early as the Oligocene.

The eastern Taranaki region exhibits a more complex oil generation history due mainly to varying amounts of subduction-related subsidence, erosion, and thrust faulting and to Quaternary magmatism. The combination of these tectonic and magmatic effects produces a transient thermal state that causes present-day surface heat flow values to vary between 50 and 70 mWm<sup>-2</sup> across the Taranaki Peninsula.

With a high initial heat flow, Rakopi Formation source rocks would have generated and expelled hydrocarbons as early as early Paleocene in regions that had rapid and excessive Late Cretaceous–Paleocene deposition (i.e. below Kapuni Deep-1). In regions where Late Cretaceous–Paleocene sediments are thinner (below Kaimiro-1) the Rakopi section may not have reached sufficient maturity until the Miocene, regardless of a high or low initial heat flow. Thus it is possible that oil may have been generated from the Rakopi section in different parts of the eastern Taranaki region for the entire Cenozoic.

Oil generation and expulsion from Paleocene–Eocene source rocks was governed by Miocene to Recent tectonics and was not affected by variations in initial conditions. In the Kapuni Deep-1 area, the Paleocene Farewell Formation (deeper than about 5500 m) is mature, with maturity sufficient for expulsion being reached as early as the Eocene. None of the Paleocene–Eocene source rock section of Kupe-1 is mature. In Kaimiro-1 and McKee-1 all of the Paleocene and parts of the Eocene source rocks are mature and probably began expelling hydrocarbons about 5–10 Ma. Generation rates decreased in the Pleistocene in McKee-1 and Kaimiro-1 due to uplift and erosion, but temperatures in the Paleocene–Eocene rocks presently are great enough for oil expulsion, especially at Kaimiro-1 where the present-day surface heat flow is relatively high.

## References

- ALLIS, R.G., P.A. ARMSTRONG, R.H. FUNNELL, & D.S. CHAPMAN, in prep., Compaction trends in the Taranaki basin, New Zealand, and implications for Neogene deformation.
- BRADSHAW, J.D., P.B. ANDREWS, & C.J. ADAMS, 1980, Carboniferous to Cretaceous on the Pacific margin of Gondwana: The Rangitata phase of New Zealand, Proceedings Fifth Int. Gondwana Symposium, Wellington, New Zealand.
- BULLARD, E.C., 1939, Heat flow in South Africa, Proc. Roy. Soc. London, Ser. A, 173, 474–502.
- BURNHAM, A.K., R.L. BRAUN, H.R. GREGG, & A.M. SAMOUN, 1987, Comparison of methods for measuring kerogen pyrolysis rates and fitting kinetic parameters, Energy and Fuels, 1, 452–458.
- BURNHAM, A.K., & J.J. SWEENEY, 1989, A chemical kinetic model of vitrinite maturation and reflectance, Geochim. Cosmochim. Acta, 53, 2649–2657.
- BURRUS, J., A. KUHFUSS, B. DOLGEZ, & P. UNGERER, 1991, Are numerical models useful in reconstructing the migration of hydrocarbons? A discussion based on the Northern Viking Graben. In: England, W.A. and A.J. Fleet (eds.), 1991, Petroleum migration, Geological Society Special Publication No. 59, 89–109.
- CHAPMAN, D.S., T.H. KEHO, M.S. BAUER & M.D. PICARD, 1984, Heat flow in the Uinta Basin determined from bottom hole temperature (BHT) data, Geophysics, 49, 453–466.
- COOK, R.A., 1987, The geology and geochemistry of the crude oils and source rocks of western New Zealand. Ph.D thesis, Victoria University of Wellington, New Zealand, 308 p.
- COOMBS, D.S., C.A. LANDIS, R.J. NORRIS, J.M. SINTON, D.J. BURNS, & D. CRAW, 1976, The Dun Mountain Ophiolite belt, New Zealand, its tectonic setting, constitution and origin, with special reference to the southern portion, Am. J. Sci., 276, 561–603.
- DUDDY, I.R., P.F. GREEN, & G.M. LASSLETT, 1988, Thermal annealing of fission tracks in apatite 3. Variable temperature behavior, Chemical Geology, 73, 25–38.
- FUNNELL, R.H., R.G. ALLIS, D.S. CHAPMAN, & P.A. ARMSTRONG, in prep., Thermal regime of the Taranaki basin, New Zealand.
- GIGGENBACH, W.F., Y. SANO, & H. WAKITA, 1993, Isotopic composition of He, CO<sub>2</sub>, and CH<sub>4</sub> contents in gases produced along the New Zealand part of a convergent plate boundary, Geochim. Cosmochim. Acta, 57, 3427–3455.
- GLEADOW, A.J.W., I.R. DUDDY, P.F. GREEN, G.M. LASLETT, & J.F. LOVERING, 1986, Confined fission track lengths in apatite — a diagnostic tool for thermal history analysis, Contrib. Mineral. Petrol., 94, 405–415.
- GREEN, P.F., I.R. DUDDY, A.J.W. GLEADOW, P.R. TINGATE, & G.M. LASLETT, 1986, Thermal annealing of fission tracks in apatite 1. A qualitative description, Chem. Geol., 59, 237–253.
- GREEN, P.F., I.R. DUDDY, A.J.W. GLEADOW, & J.F. LOVERING, 1989a, Apatite fission track analysis as a paleotemperature indicator for hydrocarbon exploration, in N.D. Naeser and T. McCulloh (eds.), Thermal History of Sedimentary Basins — Methods and Case Histories, New York, Springer-Verlag, 181–195.
- GREEN, P.F., I.R. DUDDY, G.M. LASLETT, K.A. HEGARTY, A.J.W. GLEADOW, & J.F. LOVERING, 1989b, Thermal annealing of fission tracks in apatite 4: quantitative modelling techniques and extension to geological timescales, Chemical Geology (Isotope Geoscience Section) 79, 155–182.
- HASKELL, T., 1991, An analysis of Taranaki basin hydrocarbon migration paths, some questions answered, Petroleum Exploration in New Zealand News, January, 19–25.
- HERMANRUD, C., S. EGGEN, T. JACOBSON, E.M. CARLSEN, & S. PALLESEN, 1990, On the accuracy of modelling hydrocarbon generation and migration: The Egersund basin oil find, Norway, Org. Geochemistry, 16, 389–399.
- HOLT, W.E. & T.A. STERN, in press, Subduction, platform subsidence and foreland thrust loading: the late Tertiary development of Taranaki basin, New Zealand. Submitted to Tectonics.
- HORNIBROOK, N., 1992, New Zealand Cenozoic marine paleoclimates: a review based on the distribution of some shallow water and terrestrial biota, in Tsuchi, R. and J.C. Ingle (eds.), Pacific Neogene, the environment, evolution, and events, 83–106.
- ISSLER, D.R., 1992, A new approach to shale compaction and stratigraphic restoration, Beaufort-Mackenzie Basin and Mackenzie Corridor, northern Canada, AAPG Bull., 76, 1170–1189.
- ISSLER, D.R. & L.R. SNOWDON, 1990, Hydrocarbon generation kinetics and thermal modelling, Beaufort-Mackenzie basin, Bull. Can. Petr. Geol., 38, 1–16.
- JOHNSTON, J.H., R.J. COLLIER, & J.T. CRAIG, 1988, Oil-source rock correlations in the Maui-4 exploration well, South Taranaki basin, Energy Exploration and Exploitation, 6, 233–247.

- JOHNSTON, J.H., R.J. COLLIER, & J.D. COLLEN, 1990, What is the source of Taranaki oils? Geochemical biomarkers suggest it is the very deep coals and shales, In Proc. N.Z. Oil Explor. Conf., Min. Commerce, New Zealand, 288-295.
- KAMP, P.J. & K.A. HEGARTY, 1989, Multigenetic gravity couple across a modern convergent margin: inheritance from Cretaceous extension, *Geophys. Journal*, 96, 33-41.
- KAMP, P.J., & P.F. GREEN, 1990, Thermal and tectonic history of selected Taranaki basin (New Zealand) wells assessed by apatite fission track analysis, *AAPG Bull.*, 74, 1401-1419.
- KAMP, P.J., J. NEWMAN, & I.W.S. WHITEHOUSE, 1992, Thermo-tectonic history and hydrocarbon prospectivity of Greymouth coalfield, Westland, assessed by apatite fission track analysis, In, Proc. N.Z. Oil Explor. Conf., 1991, Min. Commerce, New Zealand, 321-335.
- KILLOPS, S.D., A.D. WOOLHOUSE, R.J. WESTON, & R.A. COOK, in press, A geochemical appraisal of oil generation in the Taranaki basin, New Zealand, submitted to *Amer. Assoc. Pet. Geol.*
- KILLOPS, S.D., R.G. ALLIS, R.H. FUNNELL, & R.A. COOK, 1994, A reappraisal of the organic geochemical implications for oil generation in the Taranaki basin, In, 1994 New Zealand Petroleum Conference Proceedings. Min. Commerce, New Zealand, this volume, 308-321.
- KING, P.R., 1988, Well summary sheets, onshore Taranaki, New Zealand Geological Survey Report G125, 1-14.
- KING, P.R., 1991, Polyphase development of the Taranaki basin, New Zealand: changes in sedimentary and structural style, 2<sup>nd</sup> New Zealand Oil Exploration Conference Proceedings.
- KING, P.R., this volume, The habitat of oil and gas in the Taranaki basin, In, Proc. N.Z. Oil Explor. Conf., 1994, Min. Commerce, New Zealand.
- KING, P.R. & P.H. ROBINSON, 1988, An overview of Taranaki region geology, New Zealand, *Energy Exploration and Exploitation*, 6, 213-232.
- KING, P.R., T.R. NAISH, & G.P. THRASHER, 1991, Structural cross-sections and selected palinspastic reconstructions of the Taranaki basin, New Zealand. New Zealand Geological Survey Report G125.
- KING, P.R. & G.P. THRASHER, 1992, Post-Eocene development of the Taranaki Basin, New Zealand, Convergent overprint of a passive margin, in *Geology and Geophysics of Continental Margins*, Watkins, J. S., Zhiqiang, F., and K.J. McMillen, eds., AAPG Memoir 53, 93-118.
- KNOX, G.J., 1982, Taranaki Basin, structural style and tectonic setting, *New Zealand J. Geol. Geophys.*, 25, 125-140.
- LOPATIN, N.V., 1971, Temperature and geologic time as factors in coalification, *Izv. Akad. Nauk. SSSR., Ser. Geol.*, 3, 95-106.
- LOWERY, J.H., 1988, Catalog of vitrinite reflectance measurements and coal analyses from oil prospecting wells in Taranaki basin, New Zealand, New Zealand Geological Survey report M168.
- MACKENZIE, A.S., & T.M. QUIGLEY, 1988, Principles of geochemical prospect appraisal, *AAPG Bull.*, 72, 399-415.
- MATTINSON, J.M., D.L. KIMBROUGH, & J.Y. BRADSHAW, 1986, Western Fiordland orthogneiss: Early Cretaceous arc magmatism and granulite facies metamorphism, New Zealand, *Contrib. Mineral Petrol.*, 92, 383-392.
- PANDEY, O.P., 1981, Terrestrial heat flow in New Zealand, Ph.D. Thesis, Victoria University of New Zealand, Wellington.
- PILAAR, W.F.H., & L.L. WAKEFIELD, 1978, Structural and stratigraphic evolution of the Taranaki Basin, offshore North Island, New Zealand, *APEA J.*, 18, 93-101.
- PILAAR, W.F.H., & L.L. WAKEFIELD, 1984, Hydrocarbon generation in the Taranaki basin, New Zealand, in G. Demaison and R.J. Murriss (eds.), *Petroleum geochemistry and basin evaluation*, AAPG Memoir 35, 405-423.
- QUIGLEY, T.M., A.S. MACKENZIE, & J.R. GRAY, 1987, Kinetic theory of petroleum generation, in: Doligez, B., (ed.) *Migration of Hydrocarbons in Sedimentary Basins*, Editions Technip, Paris, 649-665.
- RIDGWAY, N.M., 1969, Temperature and salinity of sea water at the ocean floor in the New Zealand region, *N.Z. J. Marine and Freshwater Res.*, 3, 57-72.
- ROBINSON, P.H. & P.R. KING, 1988, Hydrocarbon reservoir potential of the Taranaki basin, western New Zealand, *Energy Exploration and Exploitation*, 6, 248-262.
- SASS, J.H., A.H. LACHENBRUCH, & R.J. MUNROE, 1971, Thermal conductivity of rocks from measurements on fragments and its application to heat flow determinations, *J. Geophys. Res.*, 76, 3391-3401.
- STERN, T.A., G.M. QUINLAN, & W.E. HOLT, 1992, Basin formation behind an active subduction zone: three dimensional flexural modelling of Wanganui basin, New Zealand, *Basin Research*, 4, 197-214.
- SUGGATE, R.P., 1959, New Zealand coals, *NZ Dept. Sci. Industr. Res. Bull.*, 134, 113 p.
- SUGGATE, R.P., 1974, Coal ranks in relation to depth and temperature in Australian and New Zealand oil and gas wells, *New Zealand J. Geol. Geophys.*, 17, 149-167.
- SUGGATE, R.P. & J.P. BOUDOU, 1993, Coal rank and type variation in Rock-Eval assessment of New Zealand coals, *Jour. Petrol. Geol.*, 16, 73-88.
- SWEENEY, J.J., 1990, Basinmat- fortran program calculates oil and gas generation using a distribution of discrete activation energies, *Geobyte*, April, 37-43.
- SYKES, R., R.P. SUGGATE, & P.R. KING, 1992, Timing and depth of maturation in southern Taranaki basin from reflectance and rank(S). In, Proc. N.Z. Oil Explor. Conf., 1991, Min. Commerce, New Zealand, 373-389.
- TISSOT, B.P., R. PELET, & PH. UNGERER, 1987, Thermal history of sedimentary basins, maturation indices, and kinetics of oil and gas generation, *AAPG Bull.*, 71, 1445-1466.
- THRASHER, G.P., 1990a, Tectonics of the Taranaki rift, Proceedings of the 1989 New Zealand Oil Exploration Conference, Energy and Resources Division, Ministry of Commerce, 124-133.
- THRASHER, G.P., 1990b, The Maui field and the exploration potential of southern Taranaki; a few unanswered questions, *Petroleum Exploration in New Zealand News*, July, 27-30.

- THRASHER, G.P. & J.P. CAHILL, 1990, Subsurface maps of the Taranaki basin, New Zealand, 1:500,000, 14 sheets and report, New Zealand Geological Survey Report G142.
- TULLOCH, A.J. & D.L. KIMBROUGH, 1989, The Paparoa metamorphic core complex, New Zealand: Cretaceous extension associated with fragmentation of the Pacific Margin of Gondwana.
- TULLOCH, A.J. & K. PALMER, 1990, Tectonic implications of granite cobbles from the mid-Cretaceous Pororari Group, southwest Nelson, New Zealand, *NZ J. Geol. Geophys.*, 33, 205-217.
- UNGERER, P., & R. PELET, 1987, Extrapolation of the kinetics of oil and gas formation from laboratory experiments to sedimentary basins, *Nature*, 327, 52-54.
- UNGERER, P., J. BURRUS, B. DOLIGEZ, P.Y. CHENET, & F. BESSIS, 1990, Basin evaluation by integrated two-dimensional modeling of heat transfer, fluid flow, hydrocarbon generation, and migration, *AAPG Bull.*, 74, 309-335.
- WAPLES, D.W., 1984, Modern approaches in source rock evaluation, in: Woodward, J., F.F. Meissner, and J.L. Clayton (eds.), *Hydrocarbon Source Rocks of the Greater Rocky Mountain Region*, Rocky Mountain Association of Geologists, Denver, 356-49.
- WEISSEL, J.K. & D.E. HAYES, 1977, Evolution of the Tasman Sea reappraised, *Earth Planet. Sci. Lett.*, 36, 77-84.
- WILLETT, S.D., 1988, Spatial variation of temperature and thermal history of the Uinta Basin, Ph.D. Thesis, Univ. of Utah, Salt Lake City.
- WILLETT, S.D., 1992, Modelling thermal annealing of fission tracks in apatite, in Zentilli, M., and Reynolds (eds.), P.H., *Low Temperature Thermochronology*, Mineralog. Assoc. Canada Short Course Handbook, 42-74.
- WOOD, D.A., 1988, Relationship between thermal maturity indices calculated using Arrhenius equation and Lopatin method: implications for petroleum exploration, *AAPG Bull.*, 72, 115-134.

### Acknowledgements

P. Armstrong was funded by a Petroleum Research Fund grant-in-aid administered by the American Chemical Society to D. Chapman. R. Funnell and R. Allis were funded by the Foundation for Research, Science, and Technology. P. Kamp was funded by the University of Waikato Research Committee. We are grateful for comments and reviews given by P. King, G. Thrasher, and S. Killips and the help and expertise of many people from the Institute of Geology and Nuclear Sciences. Also, this paper benefited greatly from discussions with Pat Suggate on coal rank.

### Authors

PHIL ARMSTRONG is a Ph. D candidate at the University of Utah and holds a M.Sc. from the University of Utah in structural geology. His current interests include thermal processes, basin analysis and the evolution of sedimentary basins, and the generation of hydrocarbons.

DAVID CHAPMAN is a professor of geophysics at the University of Utah. His research interests centre on thermal aspects of geological processes including the evolution of sedimentary basins.

ROBERT FUNNELL received a MSc (Physics) from Waikato University in 1983 and an MSc (Geophysics) from the University of London in 1985. As a geophysicist with the DSIR and Institute of Geological and Nuclear Sciences, he has been involved in resource exploration, with principal interests in interpretation of well log data and thermal modelling of sedimentary basins.

RICK ALLIS has been leader of the Petroleum Resources programme at the Institute of Geological and Nuclear Sciences since 1992. He received a Ph. D at the University of Toronto in 1977, and spent 12 years researching geothermal processes at the DSIR's Wairakei office. His current research interests include thermal modelling of basin evolution and the generation of oil and gas.

PETER KAMP is a senior lecturer of geology at the Department of Earth Sciences, University of Waikato, with wide interests in thermal and tectonic histories and crustal evolution. He is Leader of the Fission Track Group within the Geochronology Research Unit and has a Ph.D in stratigraphy/tectonics from the University of Waikato.